

# Modulation of Plasmonic Chiral Shell Growth on Gold Nanorods via Nonchiral Surfactants

*Xinshuang Gao,<sup>a,b</sup> Qiang Zheng,<sup>a,b</sup> Hanbo Li,<sup>a,b</sup> Chenqi Zhang,<sup>a,b</sup> Rui Cai,<sup>a,b</sup> Yinglu Ji,<sup>a</sup> Zhijian Hu,<sup>a</sup> and Xiaochun Wu<sup>\*ab</sup>*

## 1. Materials and characterization

### 1.1 Materials

Chloroauric acid ( $\text{HAuCl}_4 \cdot 3\text{H}_2\text{O}$ ) and silver nitrate ( $\text{AgNO}_3$ ) were purchased from Beijing Chemical Reagent Company (Beijing, China). L-ascorbic acid (AA) and hydroquinone (HQ) were from Alfa Aesar. Cetyltrimethylammonium bromide (CTAB), L-cysteine (L-Cys), sodium ascorbate (NaA), sodium borohydride ( $\text{NaBH}_4$ ) and 4-aminothiophenol (4-ATP) were obtained from Sigma-Aldrich. Cetyltrimethylammonium chloride (CTAC,  $\geq 97\%$ ) was from Macklin. Octadecyltrimethylammonium chloride (OTAC,  $\geq 98\%$ ), octadecyltrimethylammonium bromide (OTAB,  $\geq 98\%$ ), hydrogen peroxide ( $\text{H}_2\text{O}_2$ , 30wt%) were obtained from Aladdin. All chemicals were used as received without further purification. Deionized water ( $18 \text{ M}\Omega \cdot \text{cm}$ ) was used for preparing solution.

### 1.2 Characterization

Extinction spectra and CD spectra were obtained from Agilent Cary 60 UV-vis spectrophotometer and a JASCO J-1500 CD spectrometer, respectively, using 1 cm path-length cell. For Raman samples, extinction spectra were recorded using 1 mm path length. TEM images were recorded on a Tecnai G2 20 S-TWIN operating at an acceleration voltage of 200 kV. High-magnification TEM imaging and EDX elemental mapping were captured with a Tecnai G2 F20 U-TWIN system operating at 200 kV. Raman spectra were taken from solution phase using a Renishaw InVia Raman microscope (785 nm, 30 mW).

## 2. Experimental section

### 2.1 Synthesis of AuNR seeds and AuNR@AuAg core-shell nanostructures

#### 2.1.1 Synthesis of AuNRs with the LSPR maximum at $\sim 1000 \text{ nm}$ (AuNR1000)

AuNRs were synthesized using a seed-mediated growth method according to the reference.<sup>1</sup> Briefly, spherical Au seeds were prepared in the presence of CTAB via previous report.<sup>2</sup> The growth solution was prepared by adding HQ (0.1 M, 5 mL) into a mixture of CTAB (0.1 M, 100 mL),  $\text{HAuCl}_4$  (25 mM, 2 mL), and  $\text{AgNO}_3$  (10 mM, 4 mL). The growth of AuNRs was initiated by adding 1.6 mL seed solution into the above growth solution. The growth was continued for 12 h at 30 °C. The AuNRs were purified

by centrifugation once (9500 rpm, 15 min) and dispersed in deionized water.

### **2.1.2 Growth of AuNR@Cys50-Ag<sub>0.35</sub>Au<sub>0.65</sub> nanostructures mediated by different surfactants in the presence of Cys**

AuNR@Cys50 seeds were prepared by first dispersing AuNRs in 15 mM surfactant (CTAB,<sup>3</sup> CTAC, OTAB, or OTAC) aqueous solution at a rod concentration of 30 pM and then adding L-Cys (50 μM) and incubating at 40 °C for 1 h. To the above rod suspension, AgNO<sub>3</sub> (0.07 mM), HAuCl<sub>4</sub> (0.13 mM), and AA (0.32 mM) were added with quick shaking. The overgrowth was then conducted at 60 °C for 1 h. The sample after shell overgrowth was termed as AuNR(30)@Cys50-Sur(15)-Ag<sub>0.35</sub>Au<sub>0.65</sub>(0.2). After growth, the products were purified by centrifuging at 6500 rpm for 5 min twice.

## **2.2 Varying growth parameters for OTAC-mediated chiral growth**

The shell growth is divided into two steps. The first step is adding Cys into AuNR suspension and incubating at 40 °C for 1 h. The second step is first adding reactant reagents at given conditions to the incubation solution and then initiate grow shell at 60 °C for 1 h.

### **2.2.1 Effect of Cys incubation concentration on the shell growth of AuNR(30)@Cys(X)-OTAC(15)-Ag<sub>0.35</sub>Au<sub>0.65</sub>(0.2)**

AuNRs suspensions (30 pM) dispersed in 15 mM OTAC were incubated with different concentrations of Cys. The Cys incubation concentration was changed from 0 to 75 μM.

### **2.2.2 Varying OTAC concentration for AuNR(30)@Cys40-OTAC(X)-Ag<sub>0.35</sub>Au<sub>0.65</sub>(0.2)**

40 μM Cys was incubated with AuNRs suspensions (30 pM) dispersed in OTAC at different OTAC concentrations ranging from 0 to 100 mM.

### **2.2.3 Changing growth temperature for AuNR(30)@Cys40-OTAC45-Ag<sub>0.35</sub>Au<sub>0.65</sub>(0.2)**

The growth temperature was changed from 30 °C to 70 °C.

### **2.2.4 Varying the concentration of AuNR seeds for AuNR(X)@Cys40-OTAC45-Ag<sub>0.35</sub>Au<sub>0.65</sub>(0.2)**

AuNRs were dispersed in 45 mM OTAC with rod concentrations from 15 pM to 150 pM before incubating with 40 μM Cys.

### **2.2.5 Varying shell thickness for AuNR(60)@Cys40-OTAC45-Ag<sub>0.35</sub>Au<sub>0.65</sub>(X)**

The added concentration of AgNO<sub>3</sub> and HAuCl<sub>4</sub> was tuned from 0.05 to 0.3 mM with the fixed [Ag<sup>+</sup>] / [Au<sup>3+</sup>] molar ratio of 0.35 and [AA]/([Ag<sup>+</sup>] + [Au<sup>3+</sup>]) molar ratio of 1.6.

### **2.2.6 Varying the Ag/Au ratio of the alloy shell for AuNR(60)@Cys(40)-OTAC(45)-Ag<sub>x</sub>Au<sub>1-x</sub>(0.2)**

At the fixed total concentration of metal ions (0.2 mM) and AA concentration of 0.32 mM, [AgNO<sub>3</sub>] / [HAuCl<sub>4</sub>] percentage was changed from 10% (0.02 mM AgNO<sub>3</sub>) to 100% (0.2 mM AgNO<sub>3</sub>).

### **2.2.7 Addition of non-chiral thiol 4-ATP for AuNR(60)@Cys(40)/4-ATP(X)-OTAC(45)-Ag<sub>0.35</sub>Au<sub>0.65</sub>(0.2).**

At Cys incubation stage, a mixed solution of Cys and 4-ATP was added to AuNR

suspension by fixing Cys concentration at 40  $\mu\text{M}$  and changing 4-ATP concentration from 0 to 40  $\mu\text{M}$ .

### 2.3 Shell structure-dependent SERS response

The as-prepared samples of AuNR(30)@Cys(50)-CTAB(15)-Ag<sub>0.35</sub>Au<sub>0.65</sub>(0.2) and AuNR(60)@Cys(40)-OTAC(45)-Ag<sub>0.35</sub>Au<sub>0.65</sub>(0.2) were purified by centrifugation and then re-dispersed in 0.5 mM CTAC aqueous solution. In order to keep similar excitation intensity, the extinction value of the two samples at 785 nm was adjusted to the same value. After incubation at 30 °C for 1 h, 4-ATP (50  $\mu\text{M}$ ) solution was added and incubated at 30 °C for 3 h. The incubated suspension was put in a PDMS cuvette for Raman measurement.

### 2.4 Shell structure-dependent catalytic activity

The peroxidase-like activity of the above two chiral PNPs was detected via NaA oxidation by H<sub>2</sub>O<sub>2</sub>. NaA (50  $\mu\text{M}$ ) and H<sub>2</sub>O<sub>2</sub> (15 mM) were added in 45  $\mu\text{M}$  CTAC aqueous solution (Control), and suspensions of AuNR(30)@Cys(50)-CTAB(15)-Ag<sub>0.35</sub>Au<sub>0.65</sub>(0.2) (0.02 nM) and AuNR(60)@Cys(40)-OTAC(45)-Ag<sub>0.35</sub>Au<sub>0.65</sub>(0.2) (0.02 nM) both dispersed in 45  $\mu\text{M}$  CTAC aqueous solution. Catalytic activity was estimated using oxidation rate of NaA via its absorbance at 264 nm.

## 3. Supporting Figures

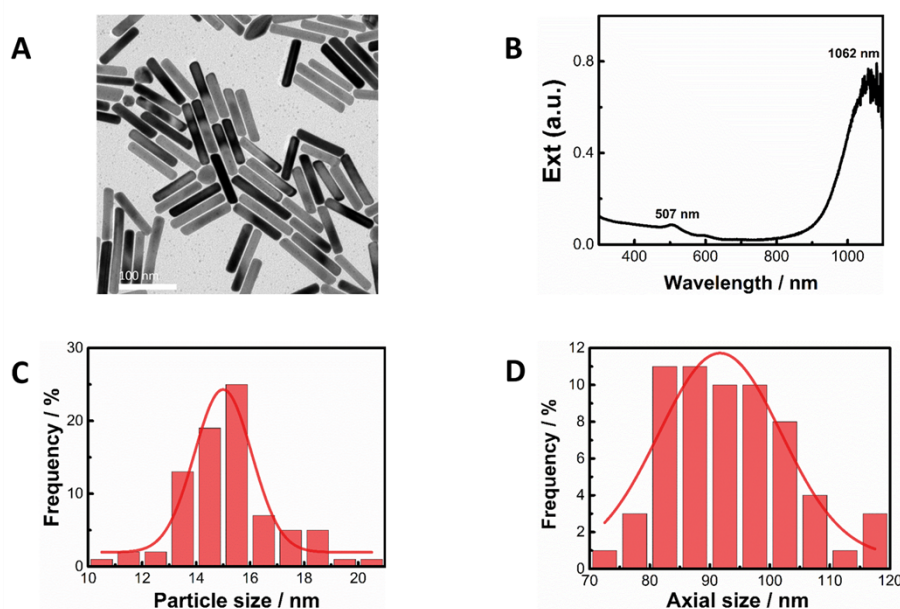


**Figure S1.** TEM image (A), extinction spectrum (B) and length and width distribution (C and D) of AuNR seeds.

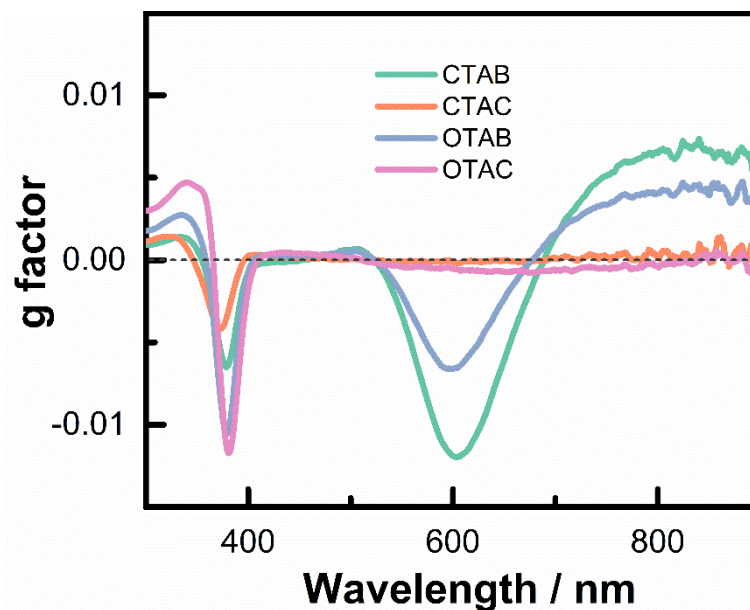


Figure S2. Corresponding g factor spectra of Fig. 1.

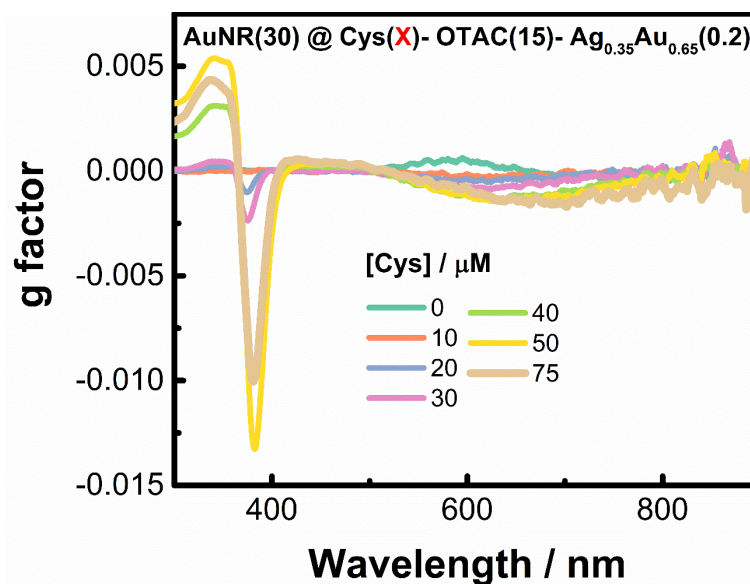
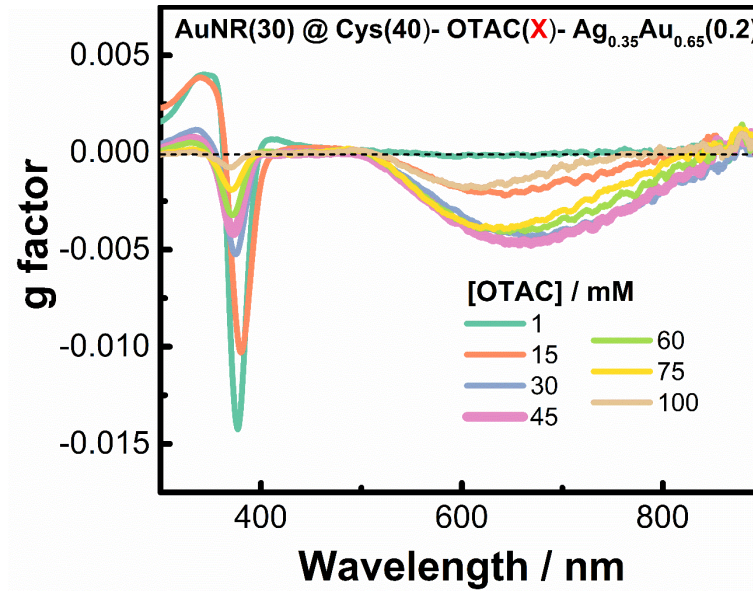
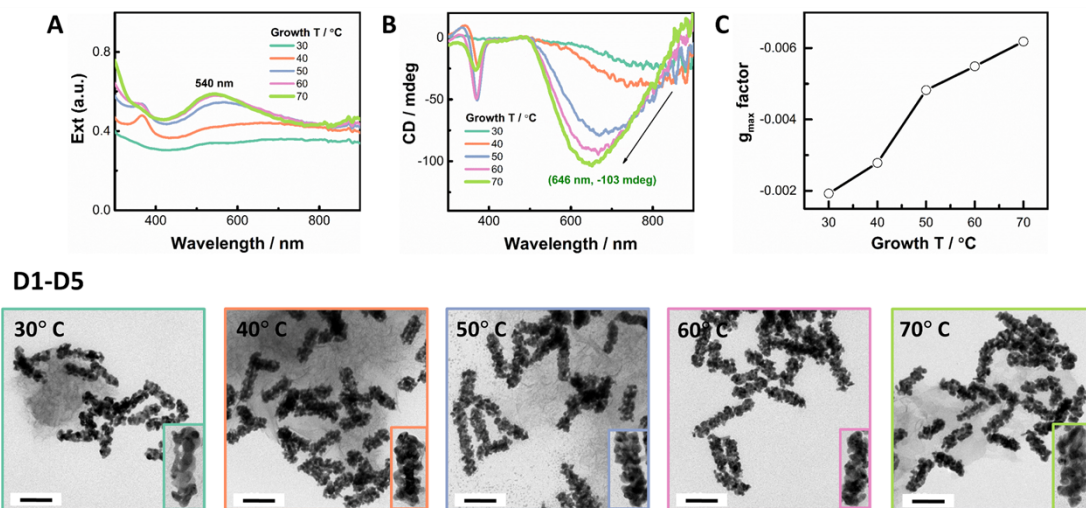


Figure S3. Corresponding g factor spectra of Fig. 2.



**Figure S4.** Corresponding g factor spectra of Fig. 3.



**Figure S5.** Effect of the shell growth temperature. Extinction spectra (A), CD spectra (B),  $g_{\max}$  vs growth temperature (C), and TEM images (D) of AuNR(30)@Cys(40)-OTAC(45)-Ag<sub>0.35</sub>Au<sub>0.65</sub>(0.2) nanostructures grown at different growth temperatures. Scale bar of the TEM images: 100 nm.

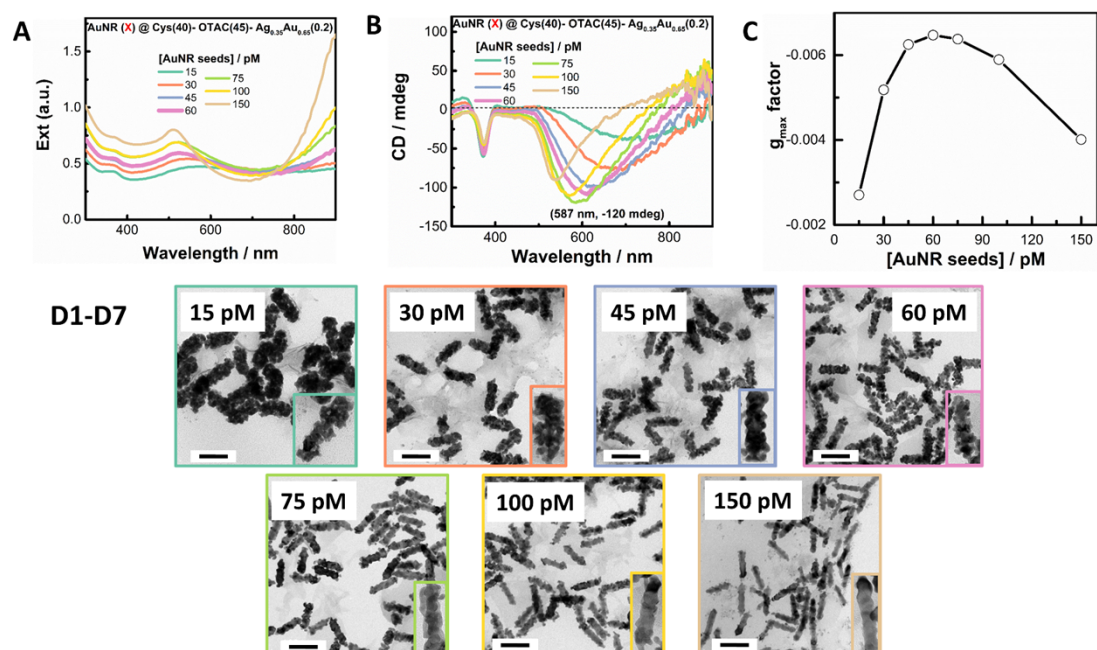


**Figure S6.** Effect of AuNR seed concentration. Extinction spectra (A), CD spectra (B),  $g_{\max}$  vs AuNR seed concentration (C), and TEM images (D) of AuNR(X)@Cys(40)-OTAC(45)-Ag<sub>0.35</sub>Au<sub>0.65</sub>(0.2) nanostructures at growth temperature of 60 °C for 1 h. Scale bar of the TEM images: 100 nm.

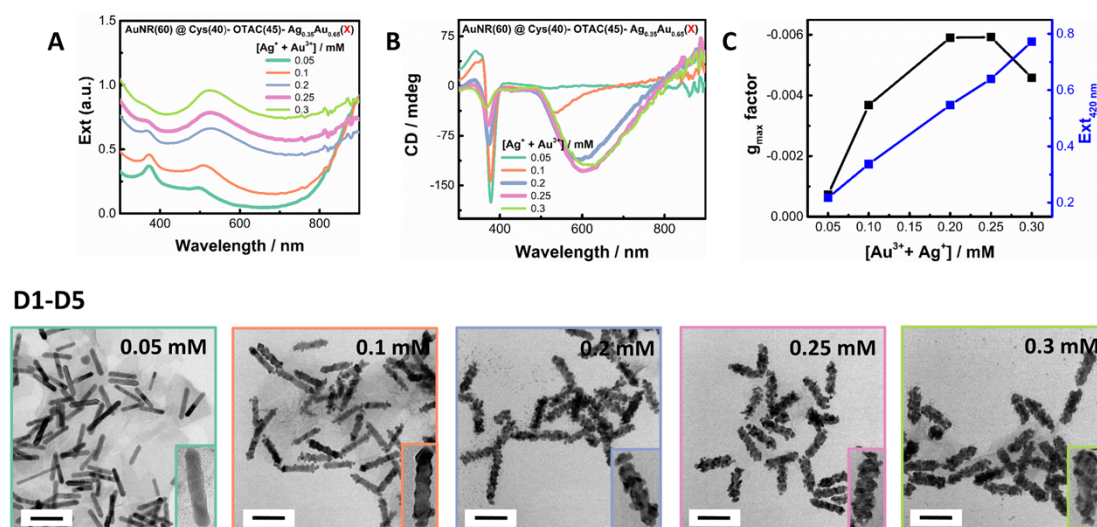


**Figure S7.** Effect of the shell thickness. Extinction spectra (A), CD spectra (B),  $g_{\max}$  and  $Ext_{420\text{nm}}$  vs [M] (C), and TEM images (D) of AuNR(60)@Cys(40)-OTAC(45)-Ag<sub>0.35</sub>Au<sub>0.65</sub>(X) nanostructures at growth temperature of 60 °C for 1 h. Scale bar of the TEM images: 100 nm.

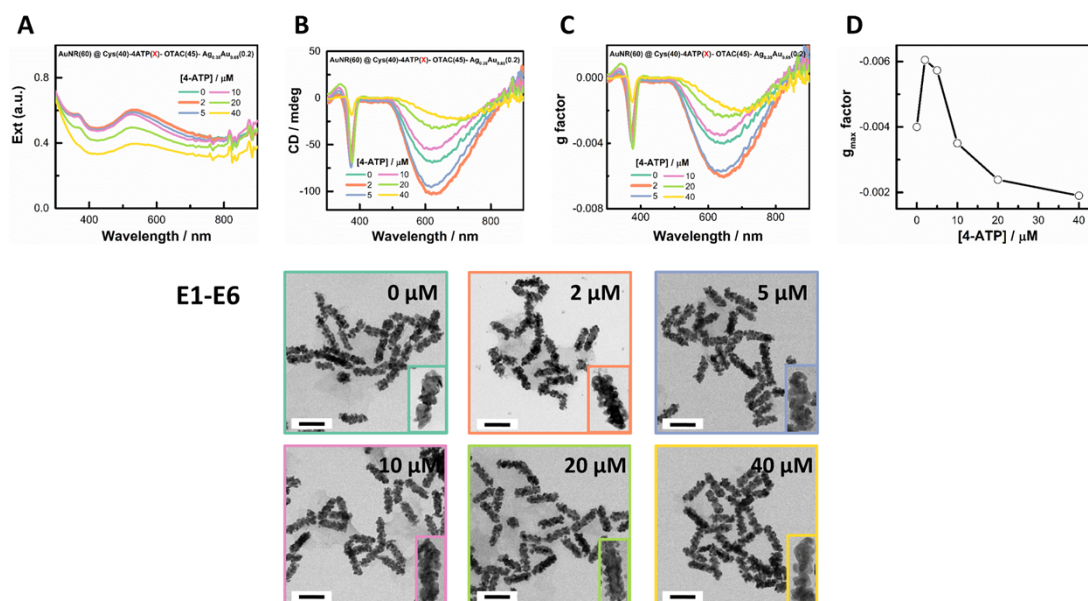


**Figure S8.** Effect of adding 4-ATP. Extinction spectra (A), CD spectra (B), g factor spectra (C),  $g_{\max}$  vs 4-ATP concentration (D) and TEM images (E) of AuNR(60)@Cys(40)-4-ATP(X)-OTAC(45)-Ag<sub>0.35</sub>Au<sub>0.65</sub>(0.2) nanostructures at growth temperature of 60 °C for 1 h. Scale bar of the TEM images: 100 nm.

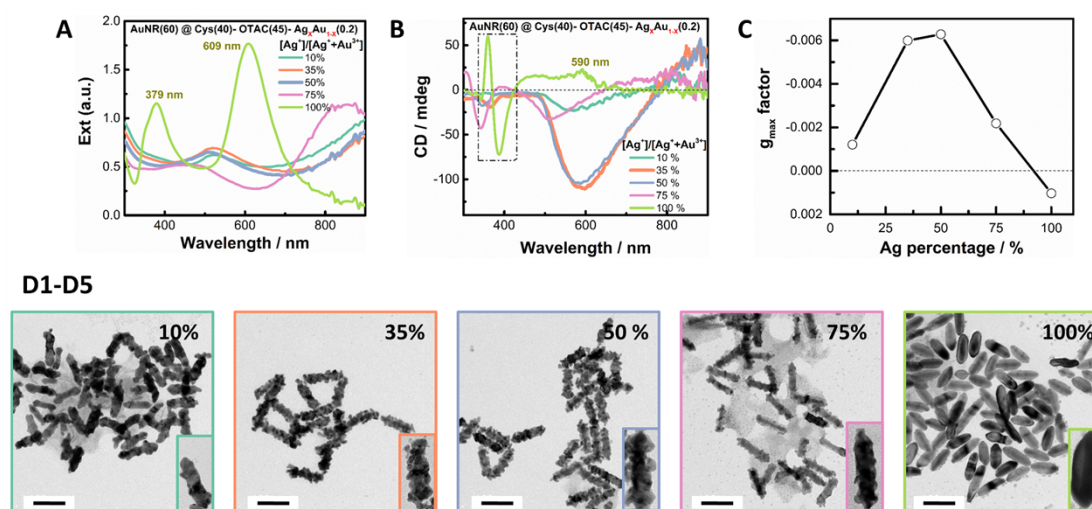


**Figure S9.** Effect of shell alloy composition. Extinction spectra (A), CD spectra (B),  $g_{\max}$  vs Ag<sup>+</sup> percentage (C) and TEM images (D) of AuNR(60)@Cys(40)-OTAC(45)-Ag<sub>x</sub>Au<sub>1-x</sub>(0.2) nanostructures at growth temperature of 60 °C for 1 h. Scale bar of the TEM images: 100 nm.

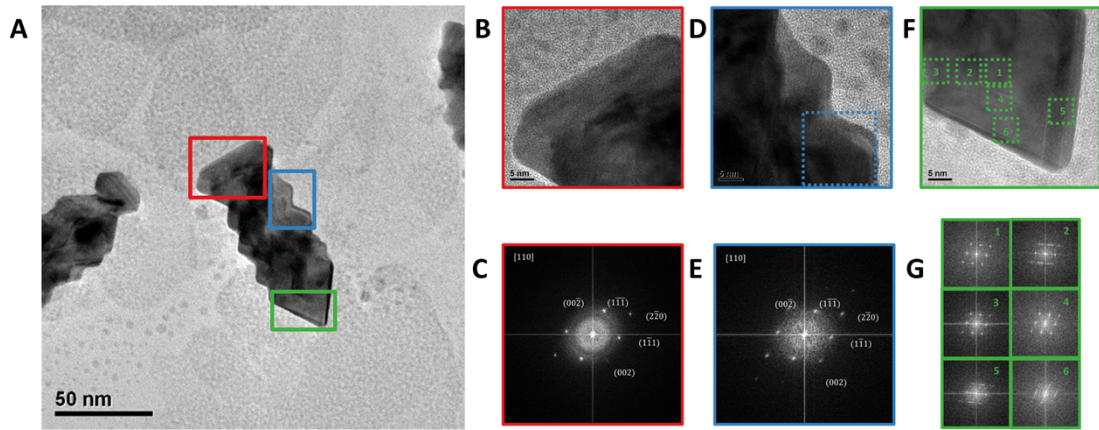


**Figure S10.** TEM characterization of AuNR(30)@Cys(50)-OTAB(15)-Ag<sub>0.35</sub>Au<sub>0.65</sub>(0.2). (A) TEM image. (B, D, F) HRTEM images marked in (A) and corresponding FFT pictures of marked regions in B, D, and F respectively.

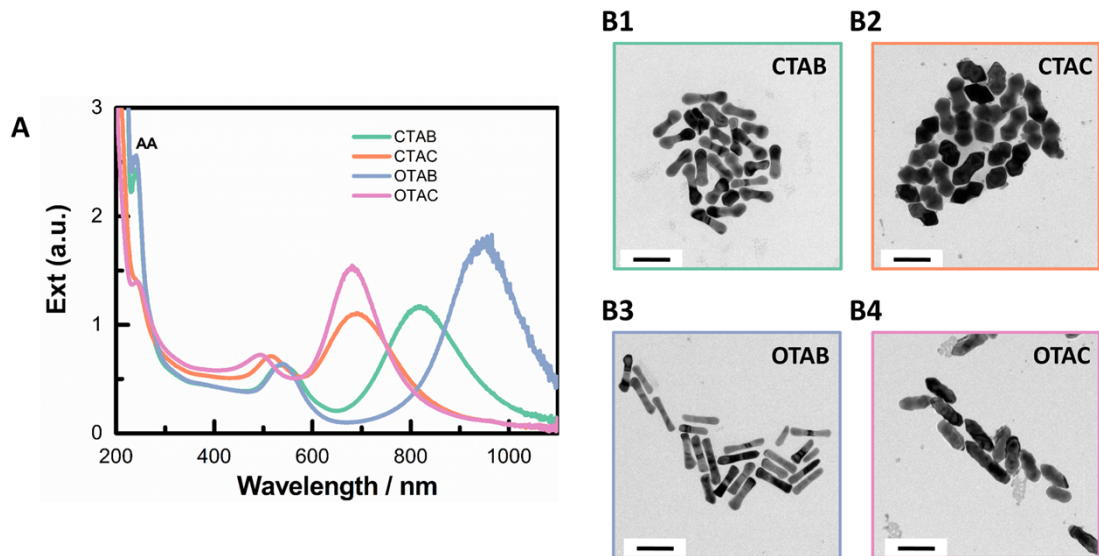


**Figure S11.** Shell growth in the absence of Cys. (A) Extinction spectra and (B1-B4) TEM images of AuNR(30)-Sur(15)-Ag<sub>0.35</sub>Au<sub>0.65</sub>(0.2) nanostructures mediated by four surfactants. Scale bar: 100 nm.

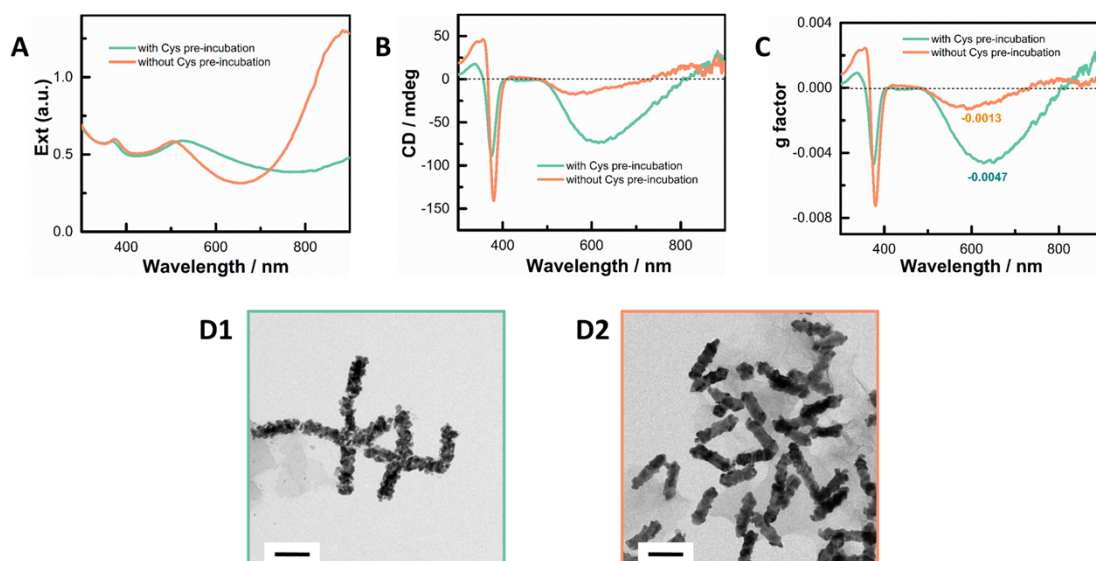


**Figure S12.** Effect of Cys pre-incubation. Extinction spectra (A), CD spectra (B), g factor spectra (C), and TEM images (D1-D2) of AuNR(60)@Cys(40)-OTAC(45)-Ag<sub>0.35</sub>Au<sub>0.65</sub>(0.2) nanostructures with and without Cys pre-incubation (40 °C 1 h) at growth temperature of 60 °C for 1 h. Scale bar: 100 nm.

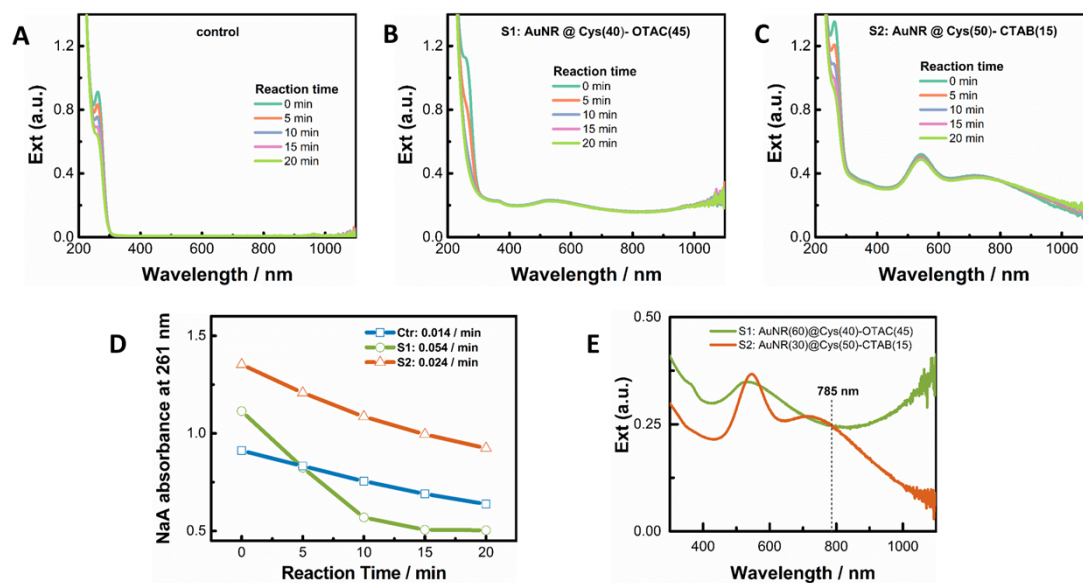


**Figure S13.** Catalytic activity of two chiral PNPs. (A-C) Evolution of absorbance spectra of control (A), S1 (B) and S2 (C). (D) NaA absorbance vs reaction time. (E) Extinction spectra of S1 and S2 used for Raman measurement.

## References:

1. L. Vigderman and E. R. Zubarev, *Chem. Mater.*, 2013, **25**, 1450-1457.
2. X. Shi, Y. Ji, S. Hou, W. Liu, H. Zhang, T. Wen, J. Yan, M. Song, Z. Hu and X. Wu, *Langmuir*, 2015, **31**, 1537-1546.
3. J. Chen, X. Gao, Q. Zheng, J. Liu, D. Meng, H. Li, R. Cai, H. Fan, Y. Ji and X. Wu, *ACS Nano*, 2021, **15**, 15114-15122.